Worcester Polytechnic Institute
Digital WPI

Major Qualifying Projects (All Years) | Major Qualifying Projects

March 2015

Design of a Plume Generation and Detection Systems

Christopher Gardner Clark
Worcester Polytechnic Institute

Madeline Divan Seigle
Worcester Polytechnic Institute

Mitchell Tanner Greene
Worcester Polytechnic Institute

Follow this and additional works at: https://digitalcommons.wpi.edu/mqp-all

Repository Citation
Clark, C. G., Seigle, M. D., & Greene, M. T. (2015). *Design of a Plume Generation and Detection Systems*. Retrieved from https://digitalcommons.wpi.edu/mqp-all/2790

This Unrestricted is brought to you for free and open access by the Major Qualifying Projects at Digital WPI. It has been accepted for inclusion in Major Qualifying Projects (All Years) by an authorized administrator of Digital WPI. For more information, please contact digitalwpi@wpi.edu.

NAG1501

Design of Plume Generation and Detection Systems

A Major Qualifying Project Report

Submitted to the Faculty of the

WORCESTER POLYTECHNIC INSTITUTE

in partial fulfillment of the requirements for the

Degree of Bachelor of Science

in Aerospace Engineering

by

Christopher Clark

Mitchell Greene

Madeline Seigle

March 23, 2015

Approved by:

Professor Nikolaos A Gatsonis, Advisor

Aerospace Engineering Program

WPI

Abstract

The project presents the conceptual design of plume generation and detection systems for ground experiments with sensing robots. The plume generation system provides controlled carbon dioxide concentration profiles and consists of a pressurized tank, a pressure regulator, a flow meter, and a nozzle placed on a stand. The carbon dioxide plume is modeled with the 3d advection diffusion equation and numerical simulations provide the required release rates at the nozzle exit. Nozzle dimensions are estimated using 1d isentropic nozzle theory. The plume detection system consists of three carbon dioxide sensors placed on a horizontal arm that can be repositioned vertically on a stand. Structural analysis is performed for the plume generation and detection stands in order to minimum deflections.

Acknowledgements

We would like to thank Professor Gatsonis for providing us with the opportunity to complete this project. We would also like to thank Tatiana Egorova and Sebastian Eslava, two graduate students at Worcester Polytechnic Institute, for their support and guidance with various aspects of the project.

Table of Authorship

Chapter 1	Seigle
Chapter 2	
2.1	Greene
2.2	Greene
2.3	Clark
2.4	Greene, Seigle
2.5	Seigle
Chapter 3	Greene, Seigle
Chapter 4	Seigle

Table of Contents

Abstract 2

Acknowledgements 3

Table of Authorship 4

Table of Contents 5

Table of Figures 7

Table of Tables 8

Chapter 1: Introduction 9

1.1 Background and Literature Review 10

1.2 Objectives and Approach 12

Chapter 2: Design of Plume Generation and Detection Systems 13

2.1 Overall Considerations 13

COZIR Sensor Specifications 14

2.2 Gas Selection 14

2.3 Estimates of Plume Profiles 15

Simulation Results 18

2.4 Design of the Plume Generation System 25

Modeling for Nozzle 27

2.5 Design of Plume Detection System 27

Chapter 3: Experiment Realization 29

3.1 Plume Generation System 29

McMaster-Carr Pressure Regulator 29

MKS Type 1179A Flow Meter 30

3.2 Plume Detection System 30

Cozir Gas Sensors 31

Chapter 4: Conclusions and Recommendations for Future Work 32

4.1 Conclusions 32

Plume Parameters 32

Plume Generation System and Components 32

Plume Detection System and Components 32

4.2 Recommendations for Future Work 33

Chapter 5: References 34

Table of Figures

Figure 1: Use of UAV's for Plume Estimation [Demetriou et al.2014 9

Figure 2. Plume Generation and Detection Experiment. 9

Figure 3: Use of ATVs for concept demonstration. 10

Figure 4: Gas Release Schematic 13

Figure 5: Plume Generation System Schematic 13

Figure 6: Example Distance Concentrations Plot 16

Figure 7: Example Line Concentrations Plot 16

Figure 8: Example Contour Concentrations Plot 17

Figure 9: Sample of Video Simulations 17

Figure 10: Simulation 1 Distance Concentrations Plot 18

Figure 11: Simulation 1 Line Concentrations Plot 18

Figure 12: Simulation 1 Contour Concentrations Plot 19

Figure 13: Simulation 2 Distance Concentrations Plot 19

Figure 14: Simulation 2 Line Concentrations Plot 20

Figure 15: Simulation 2 Contour Concentrations Plot 20

Figure 16: Simulation 3 Distance Concentrations Plot 21

Figure 17: Simulation 3 Line Concentrations Plot 21

Figure 18: Simulation 3 Contour Concentrations Plot 21

Figure 19: Simulation 4 Distance Concentrations Plot 22

Figure 20: Simulation 4 Line Concentrations Plot 22

Figure 21: Simulation 4 Contour Concentrations Plot 22

Figure 22: Simulation 5 Distance Concentration Plot 23

Figure 23: Simulation 5 Line Concentrations Plot 23

Figure 24: Simulation 5 Contour Concentrations Plot 23
Figure 25: Simulation 6 Distance Concentrations Plot 24
Figure 26: Simulation 6 Line Concentrations Plot 24
Figure 27: Simulation 6 Contour Concentrations Plot 24
Figure 28: SolidWorks Model of the Nozzle Stand 26
Figure 29: Nozzle Stand Displacement 26
Figure 30: T-Slot (http://www.parts-recycling.com/) 27
Figure 31. Plume Detection Setup 28
Figure 32: Plume detection system displacement 28
Figure 33: McMaster-Carr Two Stage Pressure Regulator (http://http://www.mcmaster.com/) 29
Figure 34: MKS Type 1179A Flow Meter (http://www.mksinst.com/) 30
Figure 35: Cozir Gas Sensor (http://www.co2meter.com) 31

Table of Tables

Table 1: Khepera IV Specifications (k-team.com). 14
Table 2: COZIR Sensor Specifications (co2meter.com) 14
Table 3: Comparison of Gases 15
Table 4: Data on Simulation Runs. 18

Chapter 1: Introduction

The detection of an accidental or intentional gas release in the atmosphere from a ground or aerial source is a crucial step in suppression of adverse effects. Unmanned aerial vehicles (UAVs) equipped with sensors can be useful in this pursuit as they have the ability to track and map a plume through the use of sensors without guidance from a human operator. A large research effort at WPI has been devoted to the use of UAVs for the estimation of plumes from moving aerial or ground sources as shown in Figure 1 (Demetriou, Gatsonis and Court, 2014; Gatsonis, Demetriou, and Egorova, 2013). In order to test and verify the approach, a ground-based experiment is designed using autonomous terrain vehicles (ATVs) operating in a closed environment with a controlled gas release as shown in Figure 2. The goal of this MQP group involves the design of experimental setups for plume generation and plume detection. The plume generation system can be used in future experiments as shown in Figure 3. The goal of a second MQP group (MAD1501) is to configure existing terrain robotic vehicles for use in future plume experiments.

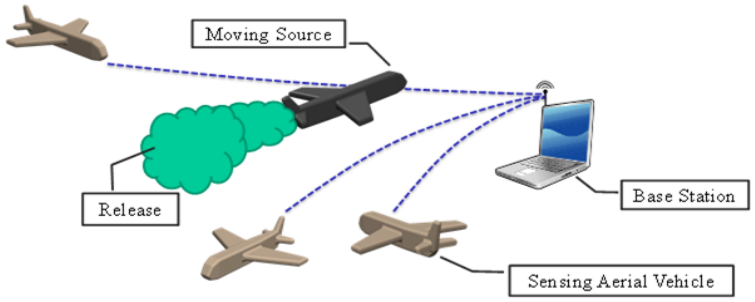

Figure 1: Use of UAV's for Plume Estimation [Demetriou et al.2014

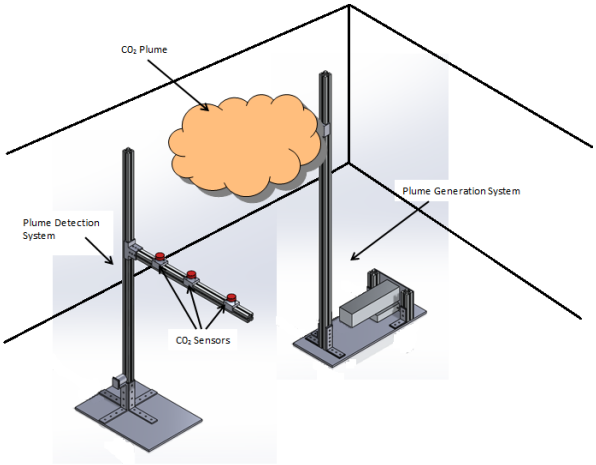

Figure 2. Plume Generation and Detection Experiment.

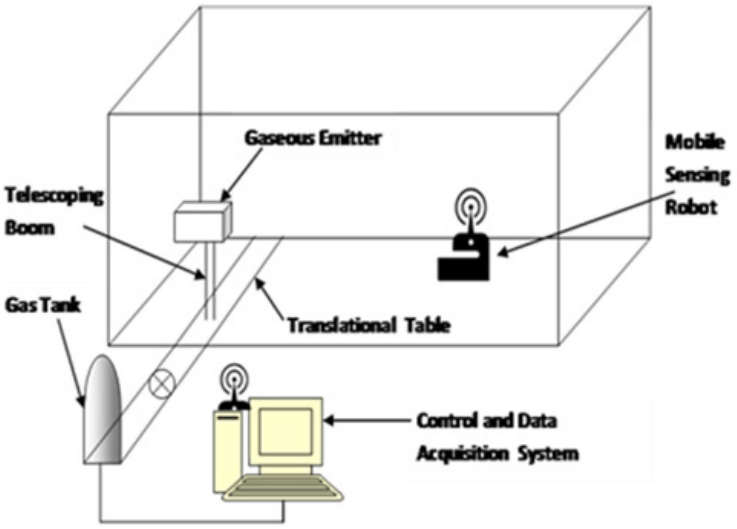

Figure 3: Use of ATVs for concept demonstration.

1.1 Background and Literature Review

There have been a number of experiments done in which an autonomous vehicle has made use of gaseous sensors to track the source of a gas release. The most relevant experiments are reviewed below, in chronological order. Though the group is focused on the plume generation system aspect of the project, the literature review takes into account all aspects of the experimental setup so as to provide a full overview of the objectives.

The team of Nakamoto et al. (1999) explored the use of a mobile robot equipped with a sensing system comprised of four tin oxide gas sensors and a wind-direction sensor to determine the location of an odor source. The wind-direction sensor consists of "four thermistor-type anemometric sensors", where the variation in response from each sensor determines the wind direction. An algorithm used to control the robot makes use of both the wind direction and the concentration gradient of the odor plume, so that the robot can stay inside the plume and make its way to the odor source. To minimize unknown variables, the experiment was conducted in a clean room with constant, known wind direction of approximately 30 cm/s from two sources. The odor source for this experiment was ethanol, chosen "for experimental simplicity", though the paper specifies that the strategies employed in this experiment can be applied to other gas/sensor combinations. The ethanol source is a nozzle 22 cm above the ground released at a rate of 75 mL/min, which the robot was able to locate in about 10 minutes at a speed of 1 cm/sec when released approximately 2-3 m from the source. Experiments in which the concentration of ethanol was lowered or the speed of the robot was increased both led to failure by the robot to locate the source, though the application of a Kalman filter led to increased success rates.

In the paper by Ishida et al. (2001), the problem approached is that of the slow recovery time of the gaseous sensors and consequential slow speed of the robot's tracking. The robot used in this experiment was equipped with 8 gaseous sensors, which, though they had high sensitivity and fast response time, required almost 30 seconds for their readings to return to normal after being removed from the gas source. Because of this, the speed that the robot can travel is highly restricted to a few meters per second and applications to systems involving faster-moving vehicles will require a new approach for the gaseous sensors. Faster sensors, such as quartz crystal microbalance sensors, give a lower sensitivity reading than that of a slower semiconductor gas sensor. The conclusions drawn include the fact that there is no sensor that is best for every situation and that there still remains a lot of work to be done regarding plume mapping and tracking.

The experiment by Hayes et al. (2002) makes use of a Moorebot in a 6.7 by 6.7 meter arena with an odor plume generated by a 23 square cm pan of hot water. The plume is dispersed by an array of 5 fans 30 cm in diameter. The Moorebot, along with gas and wind direction sensors, is also equipped with proximity sensors. The gas sensors employed are carbon-doped polymer sensors, which offer "a good combination of ease of transduction, reversibility, reproducibility, tunability, ease of production, robustness across environments, miniaturization, and speed." The sensor has a very fast response time of less than $1/10^{th}$ of a second. The wind sensor is a Shibaura F6201-1 air flow sensor with the ability to read wind flow as low as .05 m/s. To provide unidirectional sensitivity, the wind sensor is encased in a class tube. Because of this, multiple movements are required for the detection of wind direction. Simulations are done using the Webots kinematic simulator, both with a study area the same as the experimental area and one 10 times larger to verify accurate plume performance parameters. The conclusions section of this paper highlights the difficulty of obtaining real, applicable data from experimental runs due to the limited area available for testing. As in the last paper reviewed, the writers also expressed the importance of choosing gaseous plume materials and gas sensors that are the most appropriate for the given task, as there is no one option that is best for all situations.

Though paired with visual aids, an experiment by Martinez et al. (2002) uses artificial olfaction to navigate to the source of a gaseous ethanol plume and can provide insight on the plume parameters and sensors required. The sensor array on the robot makes use of two arrays, one on each side of the Koala robot, comprised of ten TGS Figaro gas sensors on each side. The sensors are grouped into five different types to attempt to compensate for the "lack of selectivity and sensitivity" of the currently available commercially available gas sensors. Despite the use of vision, the gas sensors are the primary method of gas source localization, while the use of vision is for use before the robot enters the plume.

The team of Gatsonis et al. (2013) explores the use of a dynamic grid adaptation scheme for estimating the concentration of a gaseous plume by a mobile gas sensor. The paper highlights the importance of a good control signal to the UAV in order to maximize the performance of the tracking and estimation system; in this case, the UAV is a fixed wing aircraft with concentration sensors and build in navigation capabilities. The equations that guide the SAV take into account parameters like the eddy diffusivities, wind velocities, spatial distribution, and gas release rate. The use of a dynamic grid proved to be the most effective tracking method for a released gas, with improved estimation error and results.

Demetriou et al. (2014) also works with methods for the location and tracking of a gas release. The method uses a gas dispersion model based on the advection-diffusion PDE, with ambient wind and eddy diffusivity. The paper also highlights the importance of the state estimator on the outcome of the UAV guidance, as the state estimator is used in the spatial repositioning of the UAV. The primary feature of the presented approach is the combination of estimation with CFD methods.

1.2 Objectives and Approach

The goal of this MQP group involves the design of a plume generation system and a plume detection system to be used in experiments as shown in Figure 3. The goal of the second MQP group (MAD1501) is to implement the ATVs that are to be used in the estimation process.

The objectives and approach are:

- Investigate possible gas sources and select the gas to be used in the experiments, based on health risks, availability, and cost.
- Estimate the release rate of a gas source system using a CFD model based on advection-diffusion equation.
- Design a plume generation system that includes the gas tank, pressure regulator, a flow controller, a nozzle stand, and a nozzle. The plume generation system requires the vertical re-positioning of the nozzle.
- Estimate nozzle dimensions using 1-d isentropic nozzle expansion theory.
- Design a plume detection system for three CO_2 sensors that can be positioned inside the plume and allow vertical repositioning of the sensor-arm.
- Create the plume detection system design and perform structural analysis to estimate the deflections using SolidWorks (SolidWorks).
- Identify specific parts for each component of both the probe stand and plume generation system for future construction.

Chapter 2: Design of Plume Generation and Detection Systems

This chapter presents the design of the plume experiment, including the process for choosing the gas and the method for simulating plume profiles.

2.1 Overall Considerations

One of the objectives of this project is to design experimental setups used in plume detection experiments as shown in Figure 2. The gas release tests will be conducted in an experimental area of appropriate size to allow future experiments to be conducted with the addition of ATV as shown in Figure 3. The plume generation system shown in Figure 4 must generate plumes with measurable concentrations without reaching a limit that could be dangerous to human health.

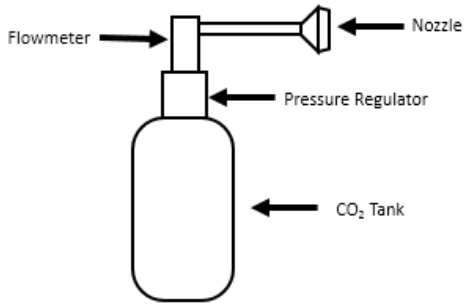

Figure 4: Gas Release Schematic

In order to ensure there will be adequate room for a plume to develop, a test area of about five meters by five meters has been chosen. For validation of the plume parameters, a plume detection system will be designed carrying three Cozir sensors as shown in Figure 5. Future experiments will utilize the Kephera IV robot equipped with four Cozir CO_2 gas sensors as the ATV in order to track and map the plume. The technical Specifications of the Khepera IV are below in Table 1 and the technical specifications of the Cozir CO_2 sensor are in Table 2.

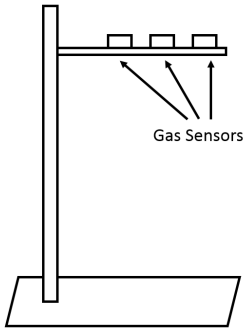

Figure 5: Plume Generation System Schematic

Khepera IV Specifications	
Elements	**Technical Information**
Processor	Linux core running on a 800MHz ARM Cortex-A8 Processor with C64x Fixed Point DSP core and additional microcontroller for peripherals management
RAM	512 MB
Flash	512 MB plus additional 4GB for data
Motion	2 DC brushed motors with incremental encoders (roughly 147 pulses per mm of robot motion) and gearbox
Speed	Max 1m/s in openloop and 0.8m/s with Factory default PID speed controller Min 0.003m/s with Factory default PID speed controller
Sensors	8 Infra-red proximity and ambient light sensors with up to 25cm range, 4 Infra-red ground proximity sensors for line following applications and fall avoidance, 5 Ultrasonic sensors with range 25cm to 2 meters, 3-axis accelerometer and 3-axis gyroscope
Audio	2x embedded microphones 1x 0.7W speaker (400-20'000Hz)
Video	Integrated color camera (752×480 pixels, 30FPS)
LED	3 programmable RGB LED on top of the robot
AC adapter power	9V @ 2.5A
Autonomy	Approximately 5 hours. Additional turrets will reduce battery life.
Battery	Embedded battery, 7.4V Lithium Polymer, 3400mAh
Docking	Ready for docking (Power input and I2C communication)
Communications	1x USB 2.0 host (500mA), 1x USB 2.0 device, 802.11 b/g WiFi, Bluetooth 2.0 EDR
Extension Bus	Expansion modules can be added to the robot using the KB-250 bus.
Size	Diameter: 140 mm Height: 58 mm
Weight	540g
Max. payload	Approx. 2000 g
Ground clearance	4 mm. Use only on hard and flat surfaces
Turn radius	0cm
Operating temperature	0-40°C
Development Environment for Autonomous Application	GNU C/C++ compiler, for native on-board applications.

Table 1: Khepera IV Specifications (k-team.com).

COZIR Sensor Specifications
Sensing Method: NDIR with Gold-plated optics
Sample Method: Diffusion / Flow with Tube adaptor
Measurement Range: 0-5%
Accuracy: ±70 ppm ± 5% of reading
Response Time Filter: 4 secs to 2 mins (user configurable) refreshed 2x/sec.

Table 2: COZIR Sensor Specifications (co2meter.com)

2.2 Gas Selection

Several different gases shown in Table 3 were evaluated according to four different criteria: safety, cost, ease of acquisition, and ease of refill. Safety considerations included flammability and asphyxiation

hazard levels. Cost includes the initial cost of the equipment, shipping costs, and gas. Ease of acquisition refers to how difficult it is to acquire the gas and any specialized parts necessary for its use, and ease of refill is how difficult it is to refill the purchased containers. Because Carbon Dioxide (CO_2) met all of our criteria, it was chosen as the best gas for our system. It is not flammable and is not considered toxic until one is exposed to 5,000 parts per million (ppm) for more than eight hours (Cdc.gov). CO_2 also has a low initial equipment cost and low refill cost. In addition, CO_2 is the easiest for the group to refill because of the close vicinity of refill stations.

	Argon	Nitrogen	Ethanol	CO_2
Safety	X	X		X
Cost		X		X
Ease of Acquisition	X	X	X	X
Ease of Refill				X

Table 3: Comparison of Gases

2.3 Estimates of Plume Profiles

In order to obtain estimates of the necessary release flow rate and duration for the plume, simulations were performed for conditions anticipated in the experiments. The code simulates in 3D the diffusion process from a source modeled via the advection-diffusion equation (Arya, 1999)

$$\frac{\partial c}{\partial t} + u\frac{\partial c}{\partial x} + v\frac{\partial c}{\partial y} + w\frac{\partial c}{\partial z} = D\left(\frac{\partial^2 c}{\partial x^2} + \frac{\partial^2 c}{\partial y^2} + \frac{\partial c^2}{\partial z^2}\right) \quad (2.1)$$

In the above Equation 2.1, $c(t, X, Y)$ is the concentration of the contaminant. The variables (u, v, w) denote the constant uniform velocity of the background wind and D is the molecular diffusivity. The model has been implemented in a simulation code using a finite-difference scheme [Demetriou et al, 2013; Gatsonis et al, 2013].

The simulation code has a simple user interface. The input variables include the full simulation time, the release time, the chamber dimensions, and the wind speed in the x, y and z-directions. The source release rate, the starting source location, and the choice between continuous or interrupted flow can also be changed. After the simulations are run, the output data is plotted using Tecplot 360 (Tecplot). Three

macros are used to plot the data in forms useful for the design of the experimental setup. After data is imported to Tecplot, the graphs generated are as shown in Figure 6, Figure 7, and Figure 8.

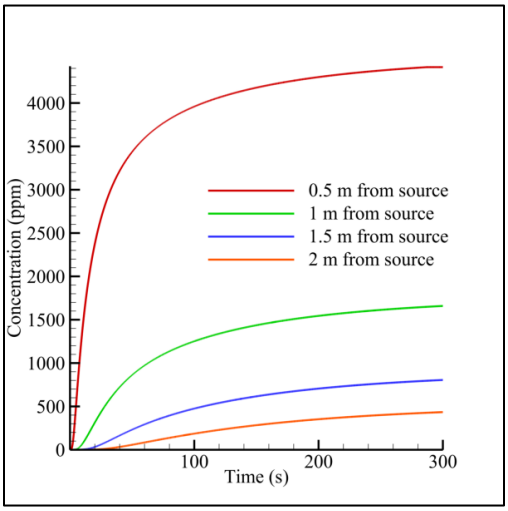

Figure 6: Example Distance Concentrations Plot

The plot in Figure 6 shows the gas concentration in parts per million over the simulation time in four locations away from the source release point. As shown in the graph legend, the lines are represented from 0.5 meters to 2 meters away from the source release point. The X-axis shows the time in seconds of the simulation from the start of the experiment to the end, while the Y-axis shows the concentration of the plume in parts per million.

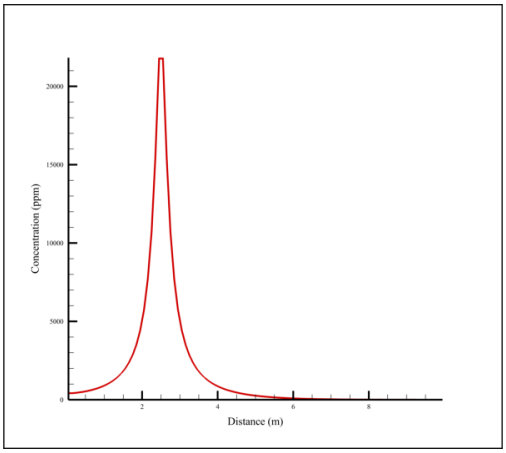

Figure 7: Example Line Concentrations Plot

The second type of plot, shown in Figure 7, shows the profile of the plume concentration in the vertical cross section of the center line of the Y-axis where the source release point is located. The X-axis portrays the distance in meters of the X-axis of the chamber. The Y-axis portrays the plume concentration in parts per million.

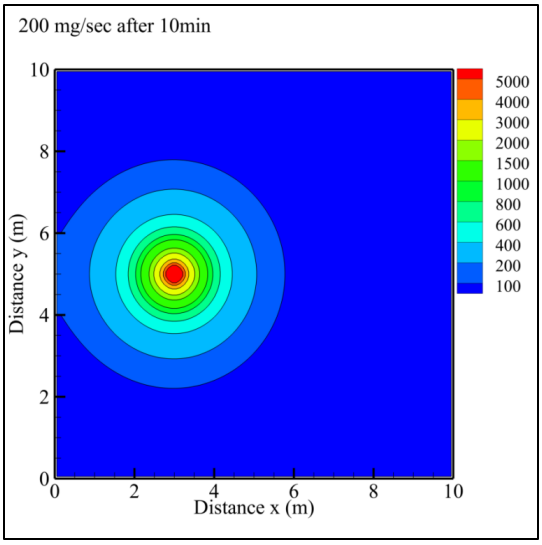

Figure 8: Example Contour Concentrations Plot

The final graph Figure 8, shows a contour plot of the horizontal cross section at the Z-direction measurement of the source release point at the end of the simulation. The different colored circles represent the different levels of concentration of the plume in parts per million as described by the legend at the right of the figure. The X and Y-axis portray the dimensions of the chamber in meters of their respective axis.

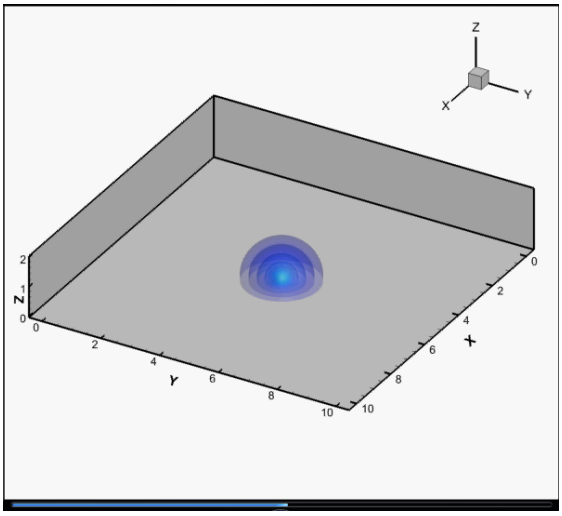

Figure 9: Sample of Video Simulations

Also possible are video simulations of the plume. In video simulations, the chamber is shown in the X-Y-Z axis. The plume outline is shown with different colored bubbles which represent the concentrations of the plume from 5 parts per million up to 30,000 parts per million. A sample still of a video simulation is shown in Figure 9.

Simulation Results

A series of simulations were performed using input parameters shown in Table 4.

Simulation Number	Flow Rate (milligrams/second)	Simulation Time (seconds)	Wind Speed (meters/second)	Continuous Flow?
1	100	600	No wind	Yes
2	100	600	(0.5, 0, 0)	Yes
3	250	600	No wind	Yes
4	250	600	(0.5, 0, 0)	Yes
5	500	600	No wind	Yes
6	500	600	(0.5, 0 , 0)	Yes

Table 4: Data on Simulation Runs.

The results for simulation 1 are shown in Figure 10, Figure 11, and Figure 12.

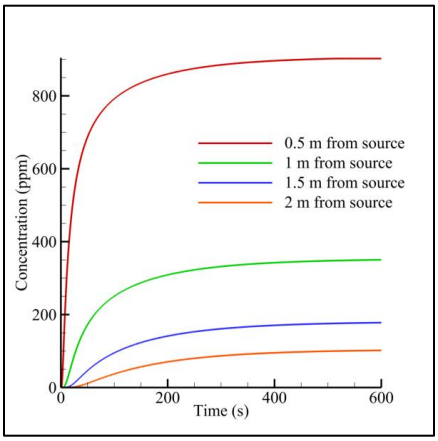

Figure 10: Simulation 1 Distance Concentrations Plot

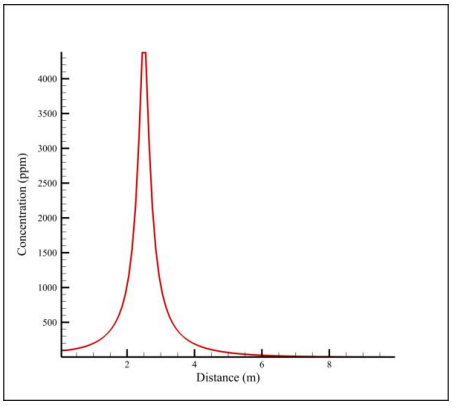

Figure 11: Simulation 1 Line Concentrations Plot

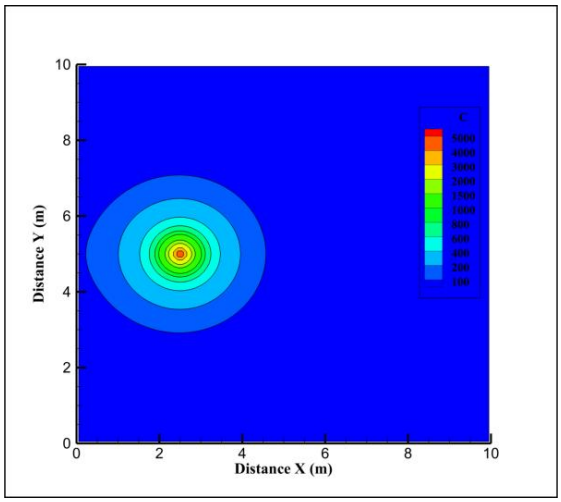

Figure 12: Simulation 1 Contour Concentrations Plot

The graphs for simulation 1 show that the concentration at the release point will be around 4400 ppm. Due to the effects of molecular diffusion, the concentration quickly drops to 900 ppm 0.5 meters away from that point. Without wind, the plume slowly continues to expand only having a diameter of 5 meters after the full 10 minute simulation.

Results for simulation 2 are shown in Figure 13, Figure 14, and Figure 15. The concentration at the release point hovers around 800 ppm and drops to 720 ppm 0.5 meters away.

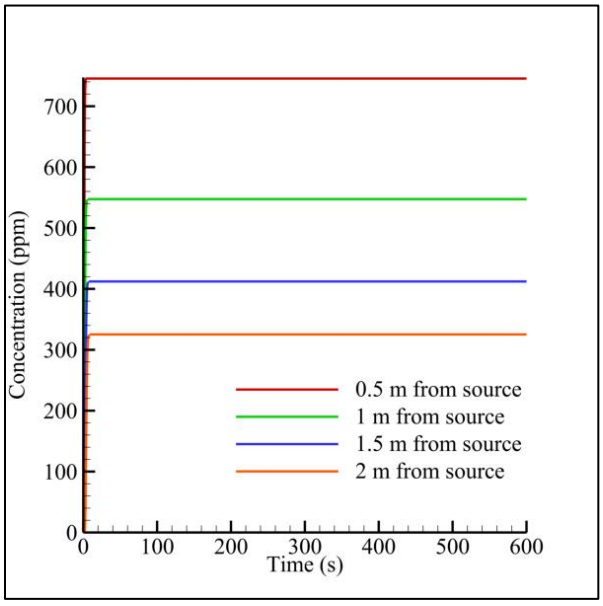

Figure 13: Simulation 2 Distance Concentrations Plot

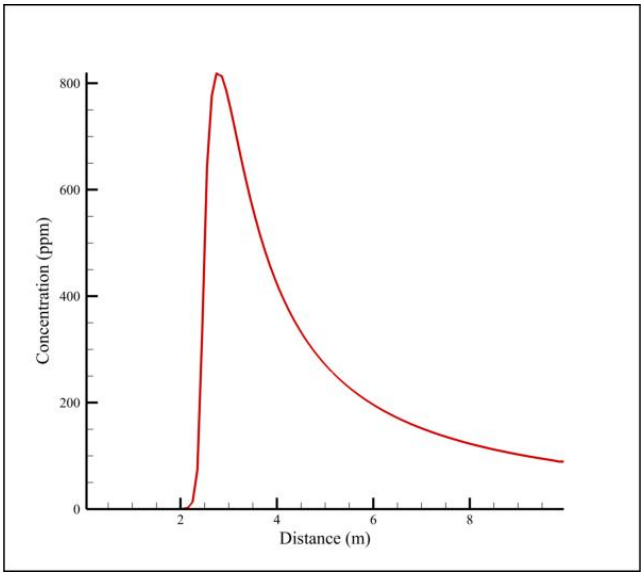

Figure 14: Simulation 2 Line Concentrations Plot

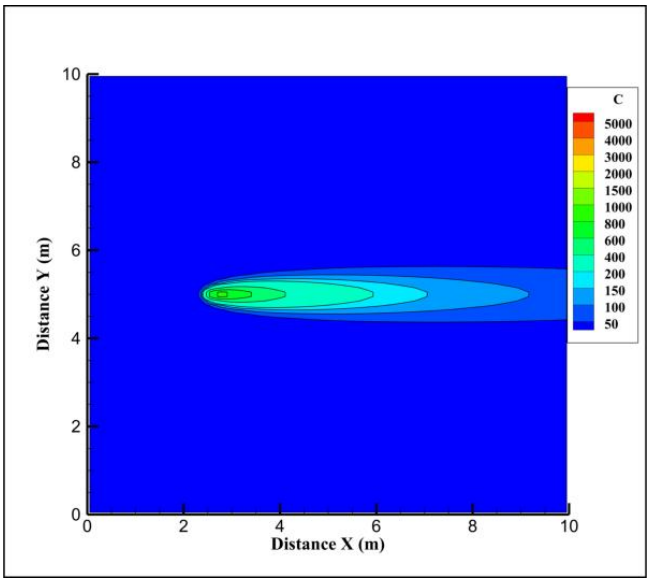

Figure 15: Simulation 2 Contour Concentrations Plot

The graphs for simulation 3 are shown in Figure 16, Figure 17, and Figure 18. The concentration at the release is around 11,000 ppm and falls to around 2,300 ppm 0.5 meters away by the end of the simulation.

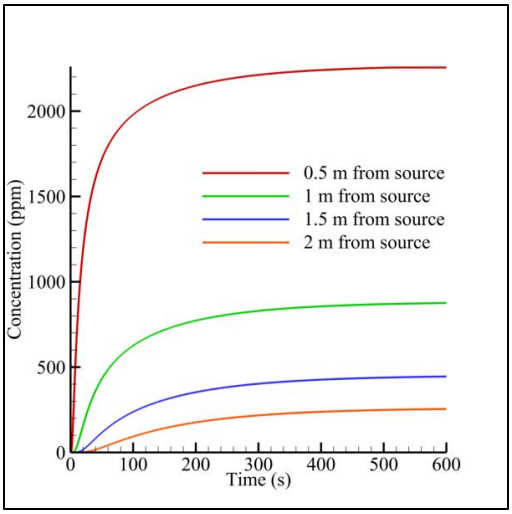

Figure 16: Simulation 3 Distance Concentrations Plot

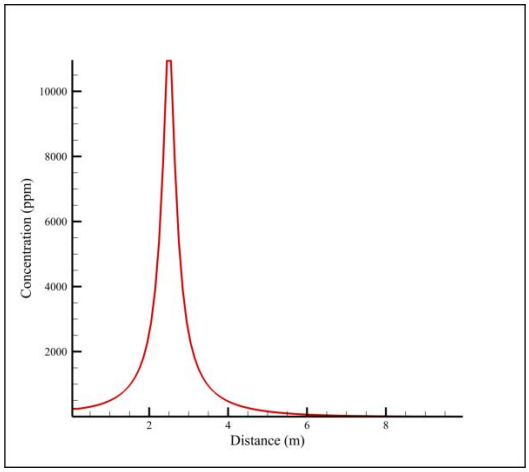

Figure 17: Simulation 3 Line Concentrations Plot

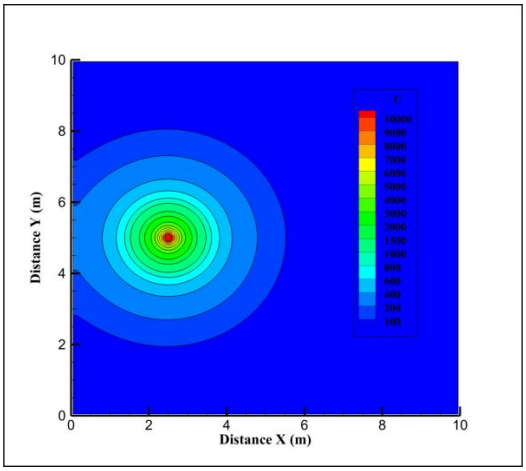

Figure 18: Simulation 3 Contour Concentrations Plot

The graphs for simulation 4 are shown in Figure 19, Figure 20, and Figure 21. The concentration at the release point is a little over 2,000 ppm while the concentration 0.5 meters away quickly goes to 1850 ppm and stays there for the duration of the simulation.

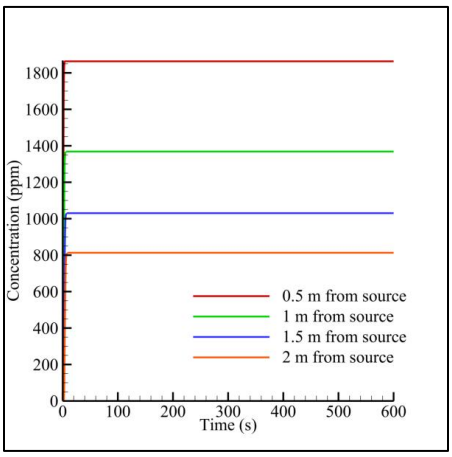

Figure 19: Simulation 4 Distance Concentrations Plot

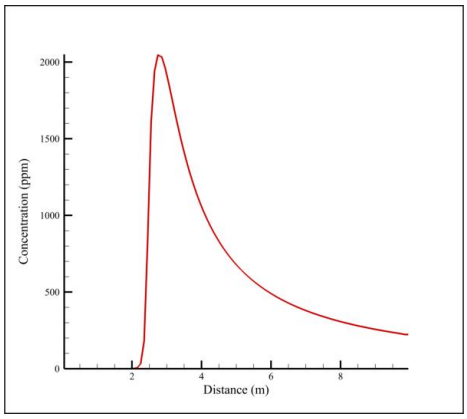

Figure 20: Simulation 4 Line Concentrations Plot

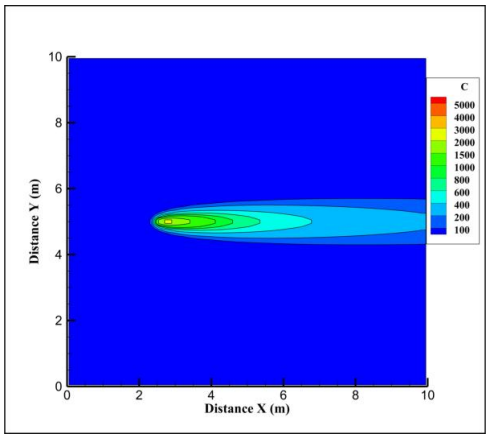

Figure 21: Simulation 4 Contour Concentrations Plot

The graphs for simulation 5 are shown in Figure 22, Figure 23, and Figure 24. The concentration at the release point is 20,200 ppm while the concentration 0.5 meters away drops to 4,500 ppm. Then 2 meters from the source the concentration falls even lower to around 500 ppm.

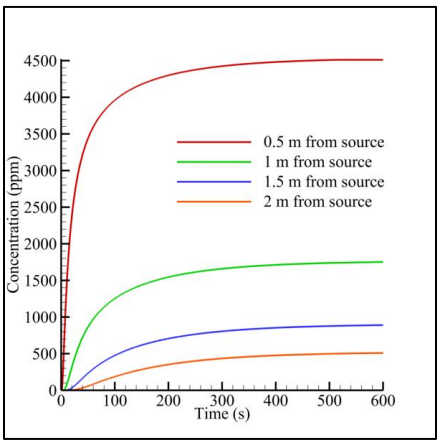

Figure 22: Simulation 5 Distance Concentration Plot

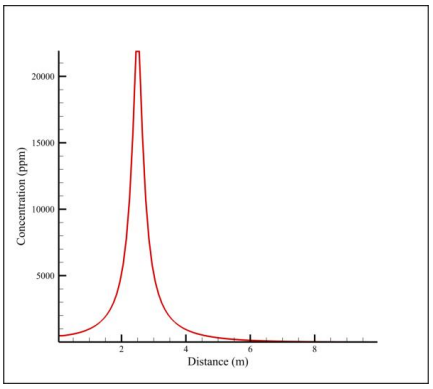

Figure 23: Simulation 5 Line Concentrations Plot

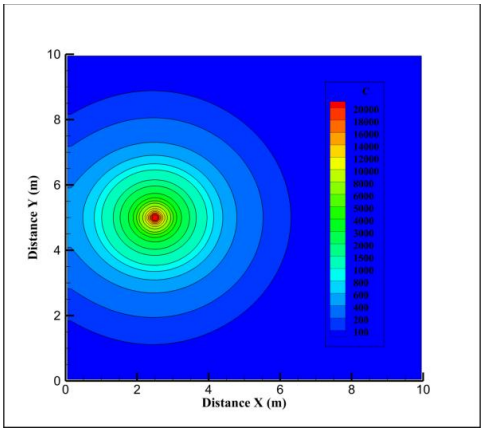

Figure 24: Simulation 5 Contour Concentrations Plot

The graphs for simulation 6 are shown in Figure 25, Figure 26, and Figure 27. The concentration at the release point is around 4,000 ppm and 0.5 meters away there is a constant concentration of 3,700 ppm.

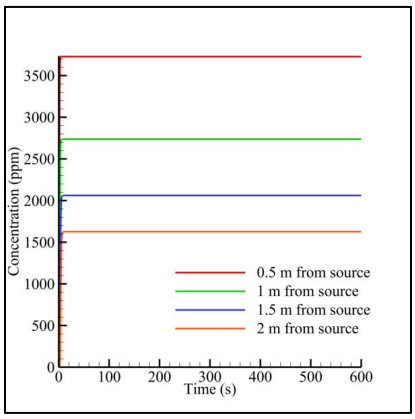

Figure 25: Simulation 6 Distance Concentrations Plot

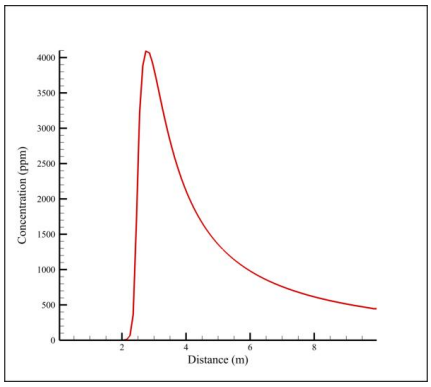

Figure 26: Simulation 6 Line Concentrations Plot

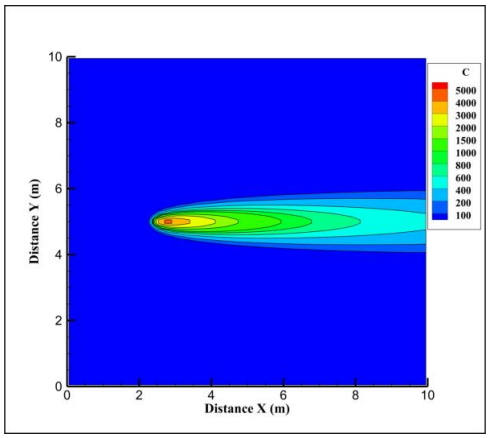

Figure 27: Simulation 6 Contour Concentrations Plot

Considering the results of the simulations several trends emerge. For a simulation with no wind the concentration at a fixed distance from the release tend to continuously increase over the duration of the simulation. When there is wind incorporated into the simulation the concentration quickly reaches a limit and stay at that concentration over the rest of the experiment. With no wind, the concentration at the release point is drastically higher than the concentrations of the trials that included wind.

The simulations provided parameters that result in plumes with concentrations safe enough for humans to be exposed to. With the use of the graphs generated in Tecplot, it is found that for a continuous gas release with no wind, flow rates between 100 and 500 milligrams per second (mg/s) are the best option for the experiment. With these conditions, the gas concentration directly at the release point is around 20,000 ppm and the concentration between 0.5 and 1 meter away from the source does not exceed 5,000 parts per million. The sensor fitted to the SAV will easily be able to detect the concentrations of carbon dioxide up to 2.0 meters from the source release point.

2.4 Design of the Plume Generation System

The source for the gaseous plume is a five-pound canister of carbon dioxide (CO_2) pressurized to approximately 700 pounds per square inch (psi). Since the pressure inside the canister decreases as the CO_2 is released, a pressure regulator is incorporated to keep the release pressure at a known, constant value. After the pressure has been decreased to approximately 100 psi it is passed through a flow meter to ensure that we are releasing the exact amount of CO_2 needed to produce a plume with specified parameters. Paired with the flowmeter will be a power supply readout so that the flowrate out of the system can be confirmed. After the flow meter there is a remotely controlled solenoid valve that allows the gas release to be terminated after a set amount of time. The final stage is a gas diffusing nozzle that will ensure the released gas diffuses uniformly around the nozzle instead of ejecting in a single direction at a supersonic velocity. Our diffusing nozzle will be located on a platform that will be able to extend or retract vertically. The full setup of the plume generation system is shown in Figure 28.

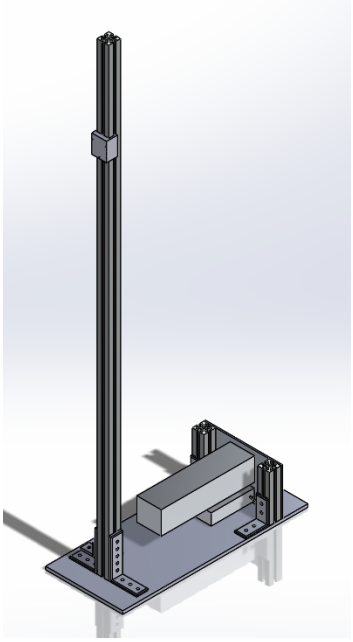

Figure 28: SolidWorks Model of the Nozzle Stand

In order to ensure that the system remains stable while in use, a static stability analysis was performed in SolidWorks, the results of which are shown in Figure 29. Though the displacement has been magnified in SolidWorks, it is confirmed that the maximum displacement of the stand is on the order of one millimeter and the system will remain stable.

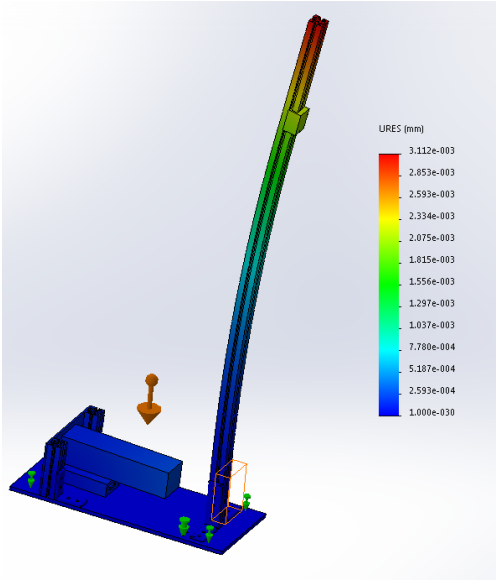

Figure 29: Nozzle Stand Displacement

Modeling for Nozzle

The primary requirement for the exit nozzle is to ensure that the flow stays subsonic; therefore, the first calculation done was to find the maximum exit pressure to keep the flow below a mach number of one using the isentropic flow relation

$$\frac{p}{p_t} = \left(1 + \frac{\gamma - 1}{2} M^2\right)^{-\frac{\gamma}{\gamma - 1}} \quad (2.2)$$

where p and p_t are the atmospheric and nozzle pressures, respectively, γ is the known specific heat constant for CO_2 of 1.28, and M is taken to be 1, the maximum exit mach number. Solving through for p_t gives us the maximum pressure at the exit to keep the flow subsonic.

In order to determine the required area ratio of the release nozzle, a Matlab code was created using the mass flowrate equation and isentropic flow relations. As previously discussed, the experiment requires a plume with a stationary source; therefore, the smallest possible velocity is needed at the nozzle. Using the previously specified mass flowrates and other known parameters, calculations were done to balance pressure, exit area ratio, and exit velocity.

2.5 Design of Plume Detection System

In order to test the validity of our plume model, the group also designed plume detection system to measure the concentration of the generated plume at various distances and heights. The probe stand of the plume generation system must have the ability to move three gas sensors in the x, y, and z directions, in order to test gas concentration in any area of the plume. The most efficient way to create a probe stand with translational abilities is to use t-slots, as shown in Figure 30.

Figure 30: T-Slot (http://www.parts-recycling.com/)

The mounting of three gas sensors on sliders along a horizontal beam of t-slot will allow for horizontal translation, while the mounting of the horizontal beam on a vertical beam of t-slot will allow for vertical translation. In order to ensure that all distance measurement is precise, proximity sensors will be

incorporated into the assembly to take readings of the x, y, and z positions of the sensors. The full setup is shown in Figure 31.

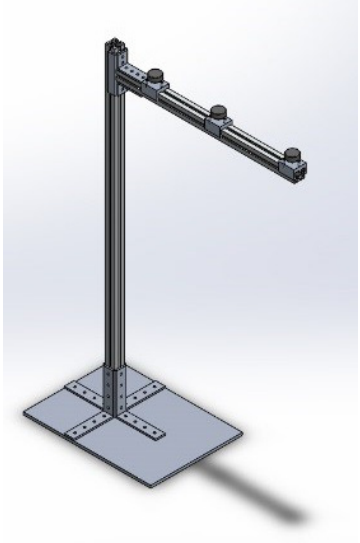

Figure 31. Plume Detection Setup

As was done with the diffuser stand, a stability analysis was also performed for the sensor stand to ensure that the horizontal bar on which the sensors are located has a displacement of no more than one millimeter for maximum plume accuracy. The results of the test are shown in Figure 32 and verify that the displacement is minimal.

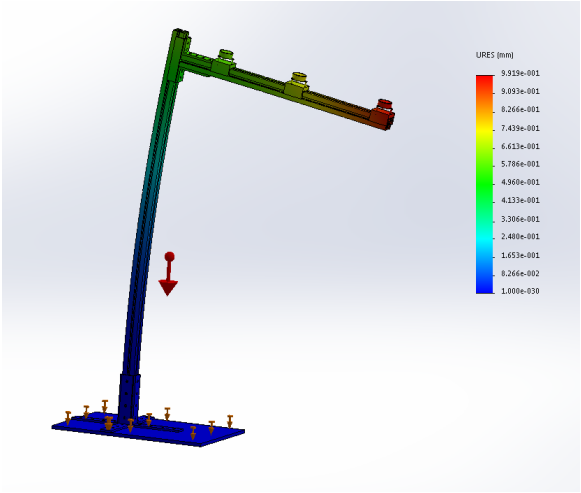

Figure 32: Plume detection system displacement

Chapter 3: Experiment Realization

This chapter explores the equipment chosen for the experiment, their features and functions, and the assembly of the system.

3.1 Plume Generation System

As outlined in Section 2.3, the plume generation system contains a CO_2 tank to act as the gas source, a pressure regulator to maintain constant pressure out of the tank, a flowmeter to guarantee we are producing the desired plume, a power supply readout to verify the flowrate, a solenoid valve to remotely turn the system on or off, and a diffuser to release the gas and create the plume uniformly. Here we examine the pressure regulator and flowmeter and the specific product that was chosen for our assembly.

McMaster-Carr Pressure Regulator

A pressure regulator works by using a pressure adjustment handle connected to a needle valve that controls how much gas passes through. A two stage regulator has two of these needle valves which decrease the pressure in two stages. The output pressure for a two stage regulator can be set and does not depend on the input pressure. In addition a two stage regulator has safety valves in case of over pressurization. We chose a two stage regulator because we need a regulator that will constantly provide a desired output pressure even with a changing input pressure from the CO_2 tank (Alspecialtygases.com). The pressure regulator the group chose is a two stage McMaster-Carr standard duty gas regulator for carbon dioxide, shown in Figure 33.

Figure 33: McMaster-Carr Two Stage Pressure Regulator (http://http://www.mcmaster.com/)

MKS Type 1179A Flow Meter

In order to keep the mass of CO_2 gas emitted constant, the group decided to use the MKS Type 1179A Mass-Flo controller, shown in Figure 34 below. The mass flow controller uses a thermal sensor in order to keep the mass of gas released constant (Mksinst.com). The thermal sensor uses the principles behind convective heat transfer in order to achieve this. The mass flow controller is comprised of two sensors. One sensor measures the temperature of the gas while the second sensor is heated. There is a change of temperature as the heated sensor is cooled by the action of molecules flowing past it and by measuring the amount of electricity necessary to keep the heated sensor at a certain temperature it is possible to measure and regulate the amount of mass flowing through it. This particular model has a 1% Full Scale and 1% reading accuracy (Sage Metering).

Figure 34: MKS Type 1179A Flow Meter (http://www.mksinst.com/)

In order to operate the MKS 1179A flow meter the experiment requires the addition of the MKS PR 4000 Digital Power Supply and Readout. The PR 4000 is vital because it allows for the flow meter to connect and be operated by a computer. The PR 4000 allows LABVIEW code to run in order to manage the amount of flow being released (Mksinst.com).

In order to run the software LABVIEW drivers must be downloaded from the website below:

http://www.pspfeifer.de/Produkte/LabVIEW_Treiber/Downloads/downloads.html

These drivers contain the necessary LABVIEW code for successful operation of the MKS 1179A and the PR 4000.

3.2 Plume Detection System

The plume detection system, as outlined in Section 2.4, is a system created with the intention of being able to measure the concentration of the plume at very precise locations. It involves a probe stand with three gas sensors, the specifics of which are discussed below.

Cozir Gas Sensors

To measure CO_2 levels our group chose the COZIR Ambient 5K CO_2 sensor. The sensor can measure CO_2 levels between 0-5000 parts per million with an accuracy of plus or minus 50 ppm. It takes two measurements a second and is based off of NDIR (NonDispersive InfraRed) technology (COZIR). The NDIR system is composed of a tube that contains an infrared light on one end that is pointing towards a detector on the other end with an optical filter in front of it. The filter blocks all wavelengths of light except for those that CO_2 absorbs. By measuring the difference in emitted light and received light the concentrations can be accurately determined (Co2meter.com). The gas sensor is shown in Figure 35.

Figure 35: Cozir Gas Sensor (http://www.co2meter.com)

Chapter 4: Conclusions and Recommendations for Future Work

Detection of a release from a ground or aerial source is a crucial step in suppression of adverse effects. Unmanned aerial vehicles (UAVs) equipped with sensors can be useful in the detection of an accidental or intentional gas release in the atmosphere. (Demetriou, Gatsonis and Court, 2014; Gatsonis, Demetriou, and Egorova, 2013). In order to test and verify the approach, a ground-based experiment is envisioned using autonomous terrain vehicles (ATVs) operating in a closed environment with a controlled gas release as shown in Figure 3. The goal of this MQP group is to design of experimental setups including a plume generation system and a plume detection system. The plume generation system will allow the creation of plumes with known parameters that can be tracked and mapped by an autonomous terrain vehicle (ATV) as shown in Figure 2. The plume detection system will be used in verification of the plumes by the plume generation system.

4.1 Conclusions

This section contains recommendations by the group on the various components of the plume dispersal system.

Plume Parameters

The project reviewed several possible plume materials, taking into consideration factors like availability, safety, and cost. Carbon Dioxide was determined to be the most appropriate gas for this experiment and should be used. After running simulations based on the 3d advection diffusion equation, it was determined that a continuous 0.005 kg/second release will provide an optimal plume with good measurability that stays below the hazardous levels for humans.

Plume Generation System and Components

The finished design for the plume generation system is presented in Section 3.1. All necessary stability tests have been performed to ensure that the stand will remain stable during use. A McMaster-Carr Pressure Regulator and MKS Type 1179A Flow Meter have been identified by the group as the pressure regulator and flowmeter that should be used in construction. Other components for construction are also identified in Chapter 3.

Plume Detection System and Components

The finished design for the plume detection system is presented in Section 3.2. Cozir gas sensors have been chosen as the most appropriate gas sensor for this application, and stability analyses has been performed on the sensor stand to ensure that the vertical deflection of the sensors is no more than 1 millimeter.

4.2 Recommendations for Future Work

The next steps in the experiment design include the fabrication and testing of the designed plume generation and detection system. Integration and testing will allow experiments to be conducted.

Chapter 5: References

Demetriou, M. A., Gatsonis, N.A., and Court, J., "A coupled controls-computational fluids approach for the estimation of the concentration from a moving gaseous source in a 2D domain with a Lyapunov-guided sensing aerial vehicle", *IEEE Transactions on Control Systems Technology*, Vol. 22, 3, pp. 853 – 867, 2014. 10.1109/TCST.2013.2267623

Gatsonis, N.A., Demetriou, M. A., and Egorova, T., "A Controls-CFD approach for estimation of concentration from a moving aerial source: comparisons between switched and dynamically adapted grids in 2D", Proceedings of the 21st Mediterranean Conference on Control and Automation, Chania, Greece, June 25-28

Cdc.gov,. 'CDC - Immediately Dangerous To Life Or Health Concentrations (IDLH): Carbon Dioxide - NIOSH Publications And Products'. N.p., 2015. Web. 3 Feb. 2015.

K-team.com,. 'Khepera IV Specifications'. N.p., 2015. Web. 3 Feb. 2015.

Co2meter.com,. 'CO2 Meter - 100% CO2 Low-Power NDIR Carbon Dioxide - Sensor By COZIR'. N.p., 2015. Web. 3 Feb. 2015.

Arya, S. P., *Air Pollution Meteorology and Dispersion*, Oxford University Press, New York, 1999.

Gonzalez, E., Mascenon, F., Magpantay, A., Go, K. and Cordero, M. (2004). Design of an Autonomous Mobile Olfactory Robot for Chemical Source Localization. *TENCON 2004. 2004 IEEE Region 10 Conference*, 4, pp.475 - 478.

Hayes, A., Martinoli, A. and Goodman, R. (2002). Distributed odor source localization. *IEEE Sensors Journal*, 2(3), pp.260-271.

Ishida, H., Nakamoto, T., Moriizumi, T., Kikas, T. and Janata, J. (2001). Plume-Tracking Robots: A New Application of Chemical Sensors. *Biological Bulletin*, 200(2), p.222.

Ishida, H., Nakayama, G., Nakamoto, T. and Moriizumi, T. (2005). Controlling a gas/odor plume-tracking robot based on transient responses of gas sensors. *IEEE Sensors Journal*, 5(3), pp.537-545.

Ishida, H., Tanaka, H., Taniguchi, H. and Moriizumi, T. (2006). Mobile robot navigation using vision and olfaction to search for a gas/odor source. *Auton Robot*, 20(3), pp.231-238.

Li, W., Farrell, J. and Card, R. (2001). Tracking of Fluid-Advected Odor Plumes: Strategies Inspired by Insect Orientation to Pheromone. *Adaptive Behavior*, 9(3-4), pp.143-170.

Marques, L., Almeida, N. and de Almeida, A. (2003). Olfactory Sensory System for Odour-Plume Tracking And Localization. *Sensors, 2003. Proceedings of IEEE*, 1, pp.418 - 423.

Martinez, D. and Perrinet, L. (2002). Cooperation Between Vision and Olfaction in a Koala Robot. *Report on the 2002 Workshop on Neuromorphic Engineering*, pp.51-53.

Nakamoto, T., Ishida, H. and Moriizumi, T. (1999). Peer Reviewed: A Sensing System for Odor Plumes. *Anal. Chem.*, 71(15), pp.531A-537A.

Russell, R., Thiel, D., Deveza, R. and Mackay-Sim, A. (2005). Controlling a Gas/Odor Plume-Tracking Robot Based on Transient Responses of Gas Sensors. *Sensors Journal, IEEE*, 5(3), pp.537 - 545.

Mksinst.com,. 'MKS Instruments - PR4000B Digital Power Supply And Readout'. N.p., 2015. Web. 10 Mar. 2015.

SolidWorks. (2014). Dassault Systems.

Tecplot. (2015). Ansys.

MAD1501, Myles, M., Angelin, M. and Hunt, M. (2015). Sensing Terrain Vehicle: Designing An Experiment for CO2 Gas Source Localization.